Chemical and Laser Cleaning of Corrosion Encrustations on Historical Stained Glass: A Comparative Study

Evan Maina Maingi [1,2,3], María P. Alonso [1], Luis A. Angurel [2,*], German F. de la Fuente [2], Stéphan Dubernet [3], Rémy Chapoulie [3], Oriane Mellouët [4] and Elodie Vally [4]

[1] Área de Historia del Arte and Unidad Asociada de I+D+I al CSIC "Vidrio y Materiales del Patrimonio Cultural (VIMPAC)", Departamento de Historia, Geografia y Comunicación, Universidad de Burgos, Po Comendadores S/N, 009001 Burgos, Spain

[2] Instituto de Nanociencia y Materiales de Aragón, CSIC-University of Zaragoza, c/María de Luna 3, 50018 Zaragoza, Spain

[3] Archéosciences Bordeaux UMR 6034, CNRS, Bordeaux Montaigne University, Espl. des Antilles, 33600 Pessac, France

[4] Maison Lorin, 46 Rue de la Tannerie, 28000 Chartres, France

* Correspondence: angurel@unizar.es

Abstract: The aim of this research work was to conduct a comparative study on the effectiveness of the application of chemical cleaning versus laser cleaning in the removal of surface congruent dissolution products from a potash-lime–silica historical stained-glass sample. EDTA was selected as the chemical cleaning agent. Laser cleaning was performed using a 238 fs pulse UV (343 nm) laser. The comparative cleaning studies were carried out on a stained-glass piece supplied by the *Maison Lorin* Glass Restoration Workshop from Chartres, France. Given the complex nature, irregular thickness and heterogeneity of the encrustations found on the glass, the two cleaning approaches were carefully performed step by step, while monitoring the process using an optical microscope. Raman spectroscopy and field emission scanning electron microscopy were used to characterize the changes induced on the sample surface during the cleaning process. The results demonstrate that the two cleaning approaches were able to eliminate the outer surface dark layer associated with carbon compounds, as well as the external part of the white layer generated by the crystallization of salts, formed with the dissolved elements after a reaction with the air. A comparison of the advantages and disadvantages of each method is also presented.

Keywords: stained glass; laser cleaning; chemical cleaning; encrustations; conservation

1. Introduction

The development of the processes for cleaning glass-based historical objects, such as stained-glass windows, is essential because the removal of encrustations, dirt and other surface contaminants ensures the restoration of these objects into a better conservation status. The cleaning process also ensures that the objects are restored back into their originally intended functionality and are more appealing from an aesthetic point of view [1–4]. Any cleaning procedure for stained-glass windows must take into account both the efficiency of the treatment and the potential harm to the material [5,6]. Therefore, prior to any cleaning procedure on historical stained glass, extreme caution should be exercised to avoid exposure and potential damage to the often delicate underlaying surfaces, since these may cause irreversible material and information loss [7,8].

The chemical composition and weathering conditions strongly determine the surface corrosive effects on historical glasses [9–12]. The CaO/K_2O molar ratio has been proposed as one of the most important parameters to determine the chemical stability of historical glasses. Potash-lime–silica glasses are the most common in medieval glasses. After the XV century, Na_2O was introduced into glass compositions in order to increase their stability.

These changes in the composition also determine the different deterioration processes when exposed to humidity, acidic or alkaline environments [1,13–16]. In the case of potash-lime–silica glasses, a usual form of deterioration is leaching or congruent dissolution in aqueous solutions [17]. When the pH < 7–9, leaching is the most important degradation process. Alkali and alkaline-earth elements diffuse towards the glass surface, while H^+ ions diffuse into the glass, generating a brittle hydrated layer on the glass surface. For higher pH values, congruent dissolution takes place. The glass network is thus perturbed, and the structure of the glass is affected, generating pits and craters. By contrast, historical soda-potash-stained glasses are commonly covered with encrustations of inorganic compounds, such as calcium carbonate and calcium sulphate, which form as a result of prolonged contact with aqueous solutions or the deposition of unwanted particles from a contaminated environment [7,13,18–23]. These encrustations require frequent removal to avoid additional damage to the glass windows, restore their functionality by improving transparency and, thus, improve the visibility of their decorated motives.

Chemical and mechanical cleaning approaches are conventional techniques for the restoration of stained-glass windows [1–3,8]. The former consists of the application of chemical methods ranging from the use of aqueous ethanol to organic solutions. These help dissolve the crusts formed either during the corrosion processes or deposited as a result of the glass being exposed to polluted environments [1–3,7,10]. Special attention must be paid, however, to avoid aggressive chemical agent actions on the glass surface being cleaned. The latter may be attacked and partially dissolved as a result of unregulated or improper pH conditions of the chemical solutions used [1,2,4,7,24,25]. Rinsing is another problem encountered with chemical cleaning, since it can be difficult to ensure the elimination of the products used. Nonetheless, the long-term presence of residues on the surface of the glass could impact its conservation. Mechanical cleaning, on the other hand, may be used as a complementary method to chemical cleaning. This is used to remove loosened surface crusts or as a stand-alone cleaning technique that uses adequate mechanical tools [3,26]. An inadequate selection of the mechanical cleaning protocol can degrade the glass by causing pits as a result of scratches, exposing the material to additional deterioration agents [3,6,27].

Laser irradiation has been introduced more recently as a new cleaning technique for the conservation of cultural heritage materials, either as a complement or as a substitute to the conventional approaches [27–33]. In the last four decades, laser cleaning of cultural heritage materials has been a subject of interest and research within the heritage conservation community [11,32,34–39]. The potential of lasers as cleaning tools for the removal of encrustations has continued to gain recognition, despite their initial limitations associated with low reliability and high costs [32,40]. In line with progressive technology improvements, extensive studies spanning from the 1980s to date have demonstrated an increased potential for the application of lasers for the safe, controllable and effective cleaning of cultural heritage materials. These included attempts at cleaning historical stained-glass windows [4,5,8,34,37,41–45]. Safe and efficient processes to clean the latter, as well as other delicate materials, have been recently enabled as a result of the most recent progress achieved in ultra-short pulse laser technology [28,34,35,37,40,46–48]. As is the case with any other restoration approach, an initial analysis of the laser–material interactions must be carried out in order to guarantee the effective cleaning without causing unwarranted damage to the glass substrates [27,32–34,49,50].

In this study, we extend the previous work related to the application of UV fs laser cleaning in soda-potash-lime–silica [37] to potash-lime–silica historical glasses. The results obtained with the chemical and laser cleaning approaches have been compared on a glass sample from the *Maison Lorin* collection (Chartres, France). The former included the application of an EDTA chelating solution, while the latter was based on the irradiation with an fs UV laser. The effectiveness of the two distinct approaches in eliminating the accumulated surface encrustations present on the stained-glass sample was evaluated. For that purpose, the surface of the glass subjected to cleaning was divided into two almost

equal halves, with the objective of studying the effects of both cleaning methods on surfaces with similar deterioration features.

2. Materials and Methods

2.1. Historical Glass Sample

In order to make comparisons between the results obtained with the chemical and laser cleaning techniques, a glass sample was provided by *Maison Lorin* Glass Restoration Workshop in Chartres, France. The glass sample was colorless, exhibited a faint greenish tint and measured approximately 8.5 cm × 6 cm. This glass sample, shown in Figure 1, was photographed under normal reflected light conditions to observe the surface morphology and assess its integrity. The selected surface corresponded to the external face that exhibited an important deterioration due to dissolution reactions (Figure 1b).

(a)   (b)
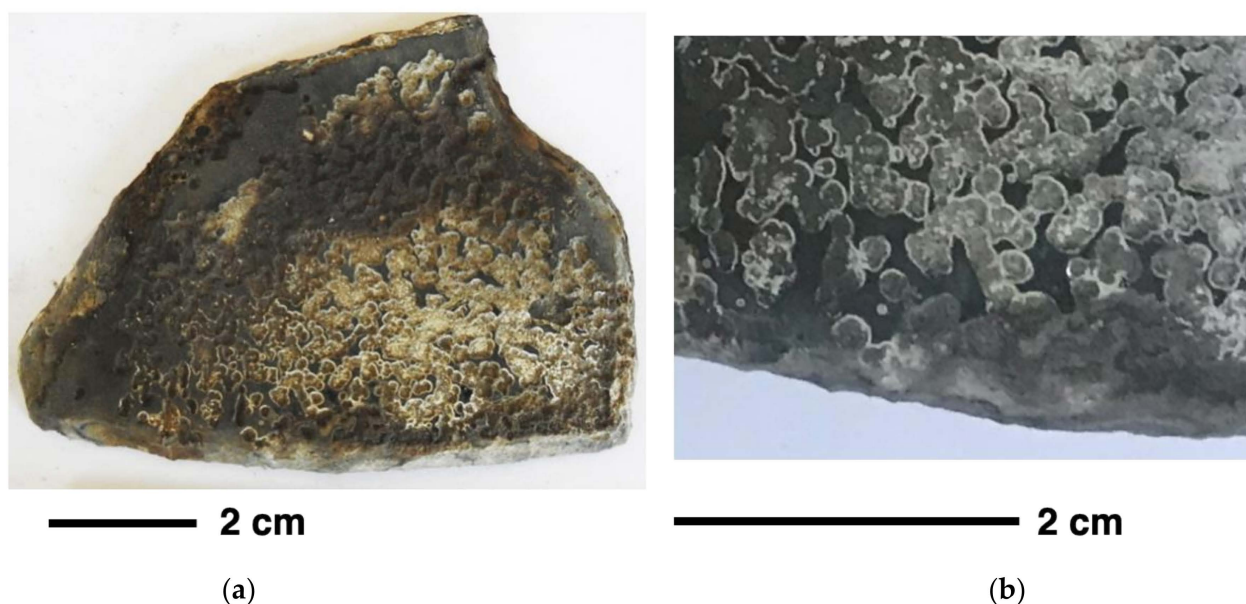
Figure 1. (**a**) Photograph of the analyzed side of the stained-glass sample used in this study. (**b**) Detail of the central bottom part showing the strong deterioration due to dissolution reactions.

2.2. Chemical Cleaning Agents

Two chemical solutions were considered as the cleaning agents to be used in the restauration of the stained-glass samples. EDTA (Ethylenediaminetetraacetic acid) and sodium thiosulfate were the compounds used to prepare the cleaning solutions. In this case, EDTA was taken as the best option. It is used to dissolve and remove the crusts on the glass surface that contains no paint/grisaille, usually the external face of the window. EDTA reacts with the oxides (iron, lead etc.) that are the constituents of the grisaille and, in consequence, its contact with the grisaille should be avoided. Basically, EDTA is prepared and applied until it no longer dissolves the crust. Usually, less than five process repetitions are required.

The solution was applied using gels prepared with Carbopol and Carbogel. Carbopol is a water-soluble polymer that is used as a suspending and thickening agent in many industries and is also used as a gelling agent. The gelling effect is activated in two steps. First, the product is dispersed in demineralized water and then hydrated. Chemicals are added in a second step in order to increase the pH. In the present case, ammonium bicarbonate was added to neutralize the solution [51]. Carbogel is made from a polyacrylic acid that has been neutralized, which allows it to form a gel when water is added. If a gel with a high viscosity is needed, Carbogel can be used in an aqueous solution. The latter has a high water retention capacity and evaporates slowly. Polyacrylic acid modified with

Carbogel can be added to EDTA to form a gel which can be applied to the glass surface requiring restoration [52].

During this study, the product was prepared by mixing EDTA with ammonium bicarbonate (20 g/L) and carbopol ultrez 21 (20 g/L) in demineralized water. The pH of the EDTA solution had to be precisely controlled in order to avoid potential damage to the glass substrate and to maximize the cleaning efficiency. For this purpose, the pH of the mixture was tested with a litmus paper. The prepared mixture was applied on one half of the glass surface and allowed to settle for approx. 2 h before being rinsed with demineralized water. The encrustation that had formed in the pits proved a challenge to remove with just a single chemical cleaning cycle. They required subsequent reapplication cycles while combining both chemical and mechanical cleaning to effectively remove the encrustation. For this reason, the process was repeated a second time.

2.3. Laser System Used in the Cleaning Process

Laser cleaning to remove the encrustations was performed on selected areas of the remaining half of the glass surface. A femtosecond (fs) UV laser (Carbide CB3-40 model with a HG (2H-3H) harmonic generator unit, Light Conversion, Vilnius, Lithuania), coupled to a galvanometer mirror system (Direct Machining Control, UAB, Vilnius, Lithuania) was employed with the selected emission wavelength at 343 nm. The maximum emission power available at this wavelength was 11 W and the pulse duration was set at 238 fs. The emission of the UV laser was chosen after an analysis of the optical response of different colored, previously selected modern stained-glass samples. The differences in the absorption between the latter glasses were found to be minimal under the UV laser, when compared to the visible and IR laser irradiation. In consequence, similar UV laser processing parameters can be selected for processing a variety of stained glass [37]. In addition, UV irradiation is much less penetrating than Vis and nIR, thus the laser-affected surface absorption layer is thinner. This enables both improved control over the ablated contaminant layer, as well as a significant reduction in the affection to the glass substrate.

Laser irradiation was performed using a beam scanning configuration with the laser beam displacement speed set at 300 mm/s and the pulse repetition frequency at 20 kHz. These processing parameters lead to a distance between the consecutive pulses of 15 µm. This same value was also selected for the interlinear distance between the two consecutive scanning lines. The glass sample was placed 4 mm below the focal working distance during the laser treatment. The laser beam size under these conditions was elliptical, with the dimensions 2a = 90 µm and 2b = 50 µm, using the $1/e^2$ criterium. The different laser cleaning protocols were explored, modifying the laser power or the energy per pulse and the number of times the laser scan process was repeated.

Laser cleaning was initially carried out on six 5×5 mm^2 regions. In the first region, the energy per pulse was gradually increased until the crust started to be removed with values lower than the damage threshold of the glass. The initial treatment revealed that the crust removal started when the laser energy per pulse reached 16.2 µJ/pulse (power, 3.24 W, fluence 0.46 J/cm^2, irradiance 1925.9 GW/cm^2). This value was very close to the minimum damage threshold measured in several modern stained-glass samples, in the range of 0.4 to 0.7 J/cm^2. Further laser cleaning was carried out under these conditions, with the laser energy level kept constant and increasing the number of irradiation scans in each region. In order to control the heat accumulation, the irradiation scans were applied in subsequent series, with each series containing a number of fixed scans. It took approximately 25 s to complete one of these series and, between the subsequent series, a time lapse of approximately 30 s was used.

2.4. Surface Analytical Techniques

The degree of degradation of the glass and the morphology of the surface before and after the cleaning interventions was examined using a portable loop microscope and a ZEISS SteREO Discovery.V8 (8:1 manual zoom range) microscope. The general morphological

aspects were documented and evaluated using photography under standard reflected light with a Canon EOS 400D digital camera. The glass surface in this study was also observed and analysed using a Field Emission Scanning Electron Microscope (FESEM, Carl Zeiss MERLIN). A semi-quantitative elemental analysis of the glass sample was performed using energy-dispersive X-ray spectroscopy (EDS, INCA350, Oxford Instruments) with acquisition times of 500 s.

Raman spectroscopy was also used for the structural investigation before and after cleaning. The equipment used in this work was a Jasco NRS 3100 equipped with two lasers, two diffraction gratings (600 and 1800 gr/mm), three objectives (5x, 20x and 100x) and a motorized stage with a step accuracy of 1 μm, a spatial resolution of 8 μm^3 and spectra resolution of 1 cm^{-1}. The spectra presented in this work were measured with the 532 nm laser and the 100x objective. A 600 gr/mm grating was used to acquire the spectra between 260 and 3600 cm^{-1}, while an 1800 gr/mm grating was selected within the 430 to 1500 cm^{-1} region.

3. Results

3.1. Original Glass Surface Observations and Analysis

The composition of the glass was determined using an EDS analysis, and the results are presented in Table 1. From the amount of K_2O (14.9 %wt) and CaO (10.3 %wt), this glass can be considered as a potash-lime–silica type.

Table 1. Composition (%wt) of the glass matrix determined using an EDS analysis in areas of 25×25 μm^2.

| %wt	SiO$_2$	CaO	Na$_2$O	K$_2$O	MgO	Al$_2$O$_3$	P$_2$O$_5$
	59.3	10.3	3.1	14.9	7.6	1.8	3.3

The observation of the glass surface under optical microscopy (Figure 2) before any cleaning interventions indicated that the main cause of damage in this glass was congruent dissolution. As observed in the optical micrographs presented in Figure 2, the glass surface morphology exhibited extensive pitting, weathering and large craters that could have formed from smaller pits increasing in size and grouping together. These craters were covered with a white, opaque layer. In addition, some areas of the surface were covered with a darker crust layer (Figure 2a). The latter were associated with the presence of carbon compounds, as confirmed by the red and blue Raman spectra presented in Figure 2c and measured on the two selected dark crust layer regions. These spectra exhibited two characteristic bands at approx. 1563 ± 10 cm^{-1}, known as the G (ordered C) band, and another band at 1360 ± 12 cm^{-1}, known as the D (disordered C) band [53]. They correspond to the red and blue curves. The red one was recorded in a region where the crust appeared directly over the glass. The blue one corresponds to a position where this carbon-compound-based crust was found on top of crystallization salts. The Raman spectra exhibited additional bands in the 600–1050 cm^{-1} range, associated with the vibration of the Si–O network on the glass. The band near 607 cm^{-1} was associated with bending vibrations, while those in the 900–1200 cm^{-1} region arose from stretching vibrations. The weak intensity of the bands in these Raman spectra suggests that the glass structure was partially destroyed [53]. The inset in Figure 2c shows an example of the broad band observed around 3400 cm^{-1}, as an indication of the hydration of the glass. The dissolution reaction promoted the formation of a modified layer that contained all the dissolved elements and that, after reaction with the air, produced the white layer that covered the glass. The band at 739 cm^{-1} can be associated with this product [54].

Additional information was obtained using a FESEM analysis. Figure 3 shows two typical regions observed on the glass surface. The aspect of the surface inside one of the craters associated with the glass corrosion process is presented in Figure 3a. The inset shows the border of one of these craters. A region of the original glass surface can be observed in the right bottom corner, showing the damage generated on the border. In these regions, an important number of cracks were detected. By contrast, Figure 3b shows a region of

the glass where the dissolution process is in an early stage, thus the glass surface is still observable, although it is covered with a crust layer. Table 2 shows the EDS analysis (%at) obtained in positions P and C, indicated in Figure 3. Additionally, the composition of the glass matrix was included for comparison. These analyses confirmed the presence of sulphur on the glass surface, suggesting its influence on the local pH changes and in the generation of the dissolution process. Figure 3b shows that these corrosion products formed a thick layer that delaminates from the glass surface in several regions. The crust layer was observed to have interacted with the glass substrate, promoting the formation of the surface cracks, as evidenced in the Supplementary Figure S1.
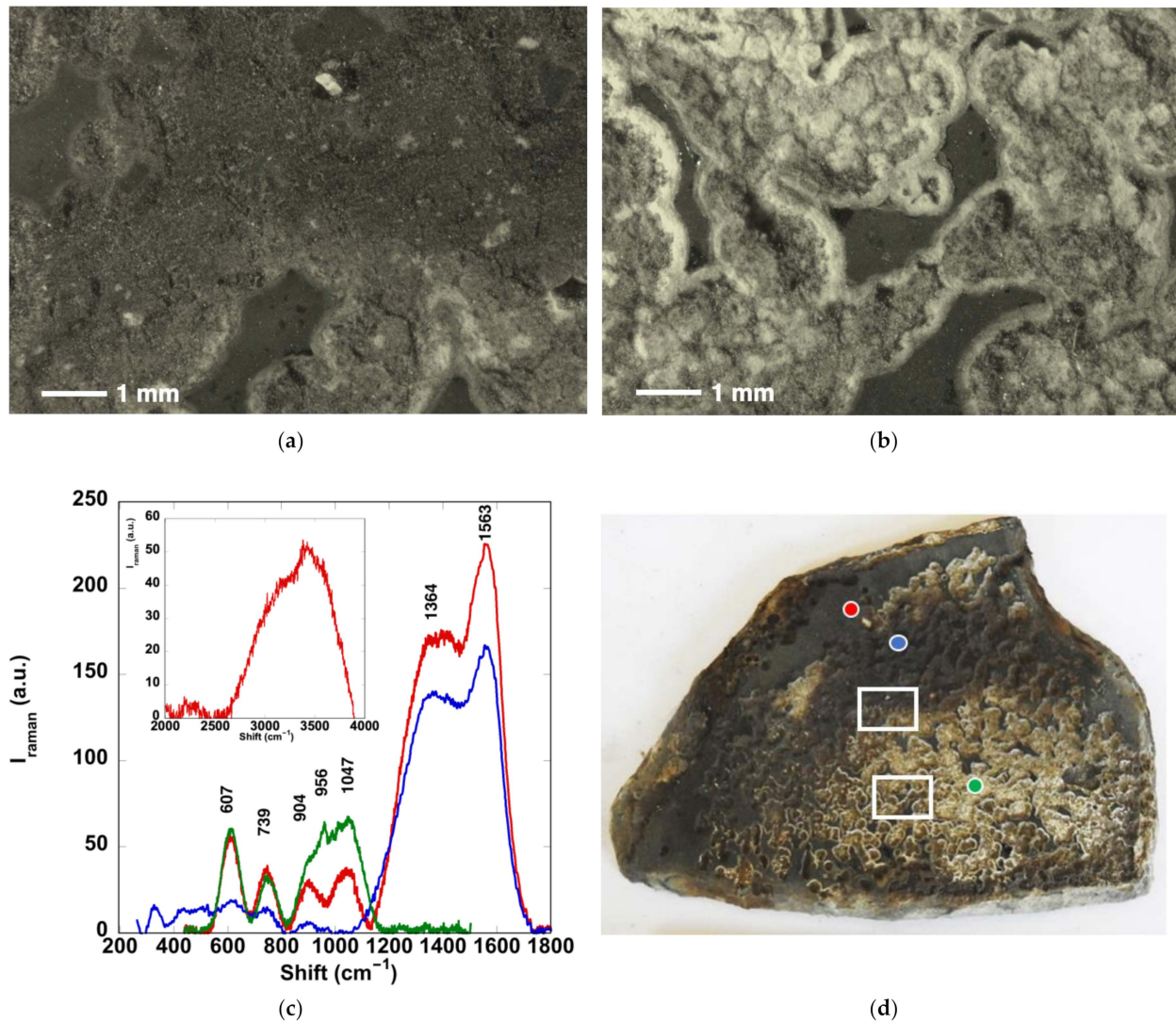
Figure 2. Optical micrographs (1×) of a region with a dark crust (**a**) and a region without this crust (**b**). (**c**) Optical micrographs (1×) of regions with (**a**) and without (**b**) a dark crust. (**c**) Raman spectra recorded in three regions showing the different surface degradation phenomena. The inset shows the 2000–4000 cm^{-1} spectrum range in a position covered with the dark crust layer. (**d**) Image of the sample showing the positions where the micrographs (rectangles) and the spectra (circles) were recorded. The color of the circles are associated to the color of the spectra in (**c**). Differences between the characteristics of the positions have been described in the text.

(**a**)

(**b**)
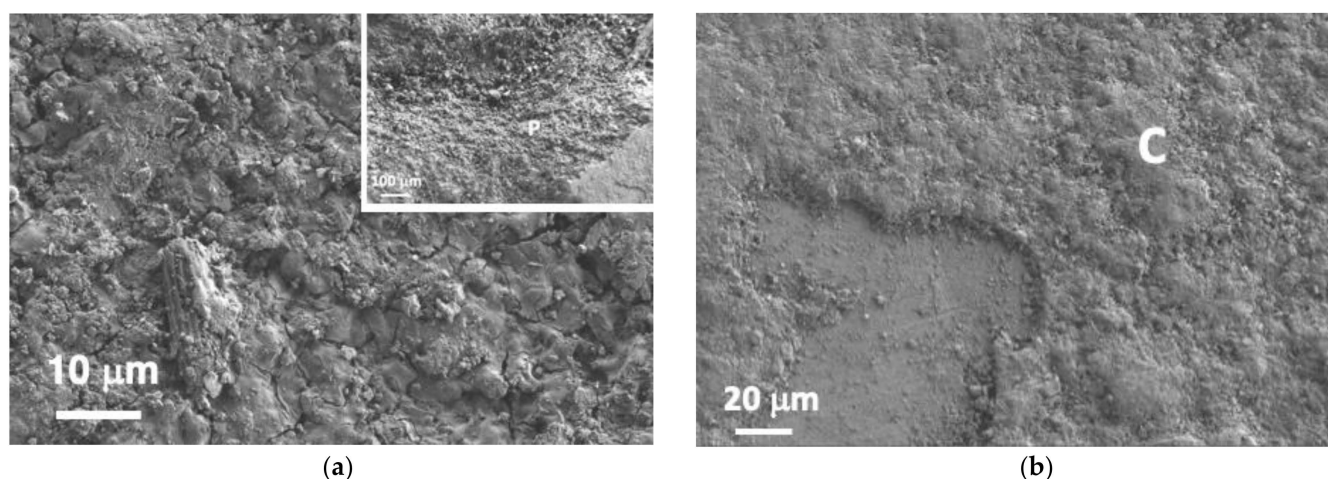
Figure 3. FESEM images of two regions of the stained-glass surface before cleaning: (**a**) a pitting corrosion region, (**b**) a glass surface covered with a corrosion crust in a region where the amount of black carbon content was low. In the inset of (**a**) a general image of the pitting corrosion region is presented. P and C indicate the positions where the EDS analysis presented in Table 2 were measured.

Table 2. EDS analysis (%at) of the composition measured in two different regions observed on the original stained-glass surface. Regions P and C are indicated in Figure 3. Comparison with the composition of the glass matrix. Measurements have been performed in the areas of 50 μm × 30 μm.

% at	C	O	Si	Ca	K	Al	Na	Mg	Fe	Pb	S	P
Crust (Region C)	25.4	51.9	13.1	2.2	0.4	2.3		0.5	1.6	0.7	1.5	0.5
Pitting (Region P)	12.3	59.6	22.9	2.3	0.4	1.0					1.1	
Glass		60.6	21.4	4.0	6.8	0.7	2.2	4.1				1.0

3.2. Chemically Cleaned Surfaces

The results after two series of chemical cleaning processes with the EDTA solution are shown in Figure 4. Comparing Figure 2a,b and Figure 4a,b, it is possible to deduce that the chemical cleaning was effective at removing the dark crust that had previously covered the surface of the glass. This fact was confirmed by the Raman spectra presented in Figure 4c. The two bands associated with the carbon compounds (1364 and 1583 cm^{-1}) disappeared and only the bands associated with the degraded glass (610, 745, 904 and 1044 cm^{-1}) were present in the spectra. The red curve was recorded on top of a region where the glass corrosion appeared to be less intense. This region corresponds to the glass observed in the right part of Figure 4a. The Raman band intensity was higher in comparison to the spectra measured in the regions before cleaning (Figure 2c). By contrast, when the spectrum was acquired inside a crater (blue line), the band intensity was similar to that observed in the sample before cleaning. These observations suggest that the amount of crust on top of the glass is reduced during the cleaning process. The EDS measurements were performed inside a crater (pitting region) and on top of the glass (crust region), and the results are presented in Table 3. The main difference in comparison to the similar results in the surfaces before cleaning (Table 2) was the strong reduction in the C content in the regions that were covered with the black layer before cleaning.

The FESEM micrographs, presented in Figure 5, correspond to the surface of the chemically cleaned glass. Figure 5a shows the surface inside one of the craters of the pitting region. The external layer that was observed in the sample before cleaning (Figure 3a) has been removed and the micrograph reveals the presence of ca. 10 μm size particles. Figure 5b shows a representative micrograph, where the surface of the glass appears to have suffered

a lower level of degradation. The crust layer that covers the glass exhibits a smoother surface finish, confirming the elimination of the external carbon contaminant particles.
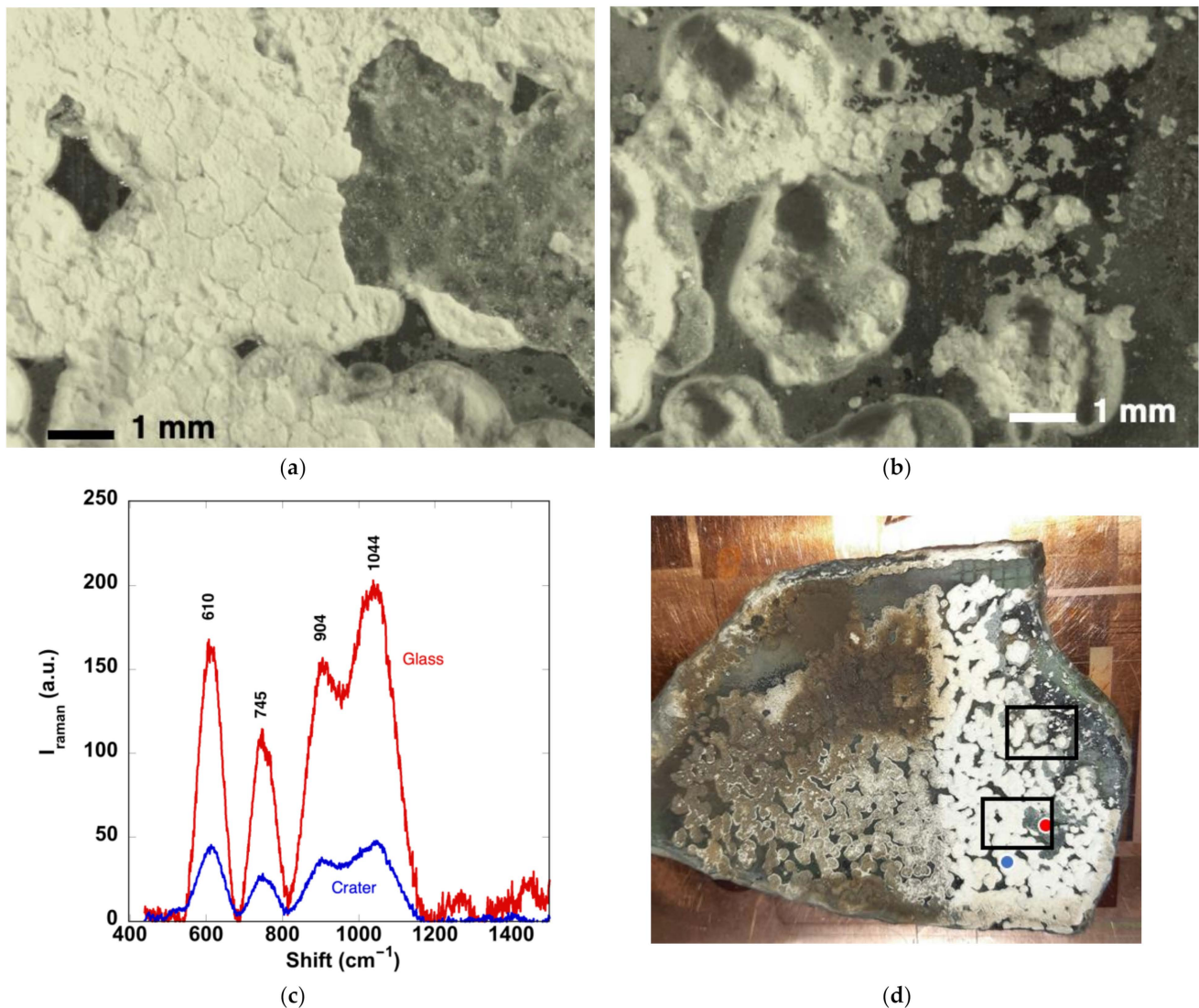
Figure 4. (**a**,**b**) Optical micrographs (1×) showing the aspect of the glass surface after chemical cleaning with the EDTA solution. (**c**) Raman spectra recorded on top of the glass and inside a crater. (**d**) Photograph of the sample showing where the images (**a**,**b**) were recorded and the points where the Raman spectra were acquired. The color of the circles are associated to the color of the spectra in (**c**). Differences between the characteristics of the positions have been described in the text.

Table 3. EDS analysis (%at) of the composition measured in two regions observed on the chemically cleaned stained-glass surface. Measurements were performed within the areas of 270 μm × 200 μm.

| % at	C	O	Si	Ca	K	Al	Mg	Fe	Pb	S	P
Crust region	14.0	57.6	21.0	1.4	0.5	2.7	0.3	1.3	0.5	0.7	
Pitting	13.5	57.8	26.9	0.7		1.1					

(**a**)   (**b**)
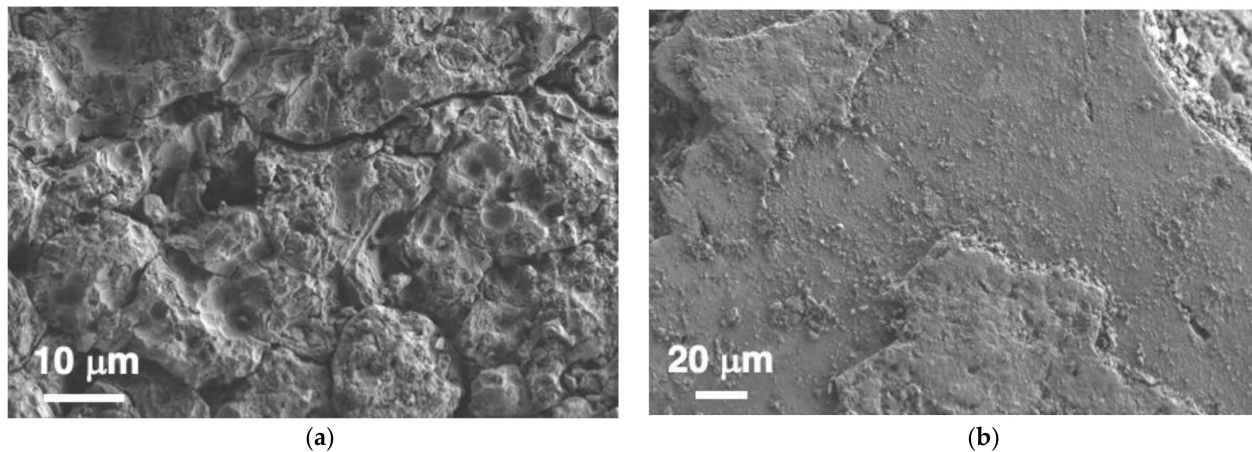
Figure 5. FESEM images of (**a**) a surface inside a crater and (**b**) of the upper glass after chemical cleaning with the EDTA solution. The magnification is the same as in Figure 3.

3.3. Laser-Cleaned Surfaces

Laser cleaning was initially carried out on six 5×5 mm^2 regions, as described in Section 2.4. Figure 6 shows an image of the sample with the exact position of these six regions as well as some optical micrographs of each of these regions. During these initial laser cleaning treatments, the number of laser scans was modified, as indicated in Table 4.
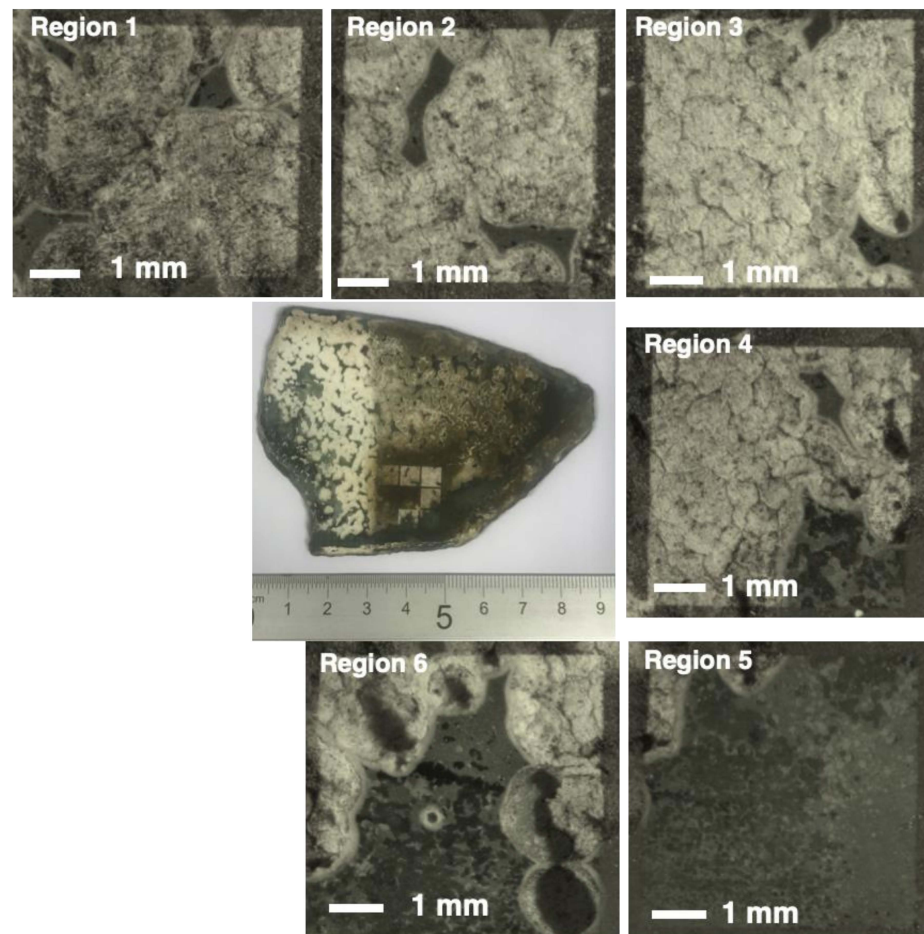

Figure 6. The six selected regions for laser cleaning with the fs UV laser and the optical micrographs (1×) of the aspect of the surface after the application of the cleaning protocol described in the text.

Table 4. Number of scans applied in the six selected regions treated with the UV fs laser and presented in Figure 6.

	Region 1	Region 2	Region 3	Region 4	Region 5	Region 6
Number of scans	5	20	100	20	20	50

In Region 1, the preliminary laser cleaning of this glass began with a single series of five irradiation scans. The black crust was partially removed with this number of series, as shown in Figure 6 (Region 1). There were no observable signs of damage to the glass substrate. Subsequently, in Region 2, the number of irradiation scans in a series was increased up to 20. The resultant laser cleaning procedure was more effective in the crust removal under these conditions, with no signs of damage to the glass substrate. The number of irradiation scans was further increased to a total of 100 times in Region 3. The dark crust was completely and effectively removed, exposing a white-colored crust layer.

These changes on the glass surface were also confirmed by the FESEM observations, as observed in Figure 7a. The surface seemed to be more uniform without the characteristic particles associated with the carbon compounds. In addition, in the regions that were not affected by pitting, the amount of crust removed from the glass surface increased in a similar fashion to chemical cleaning. The Raman spectra (Figure 7b) also correspond to the measurements recorded in specific surface regions. The main Raman bands were associated with the degraded glass in all cases, although additional bands associated with carbon compounds or other secondary phases were also identified.

(**a**) (**b**)
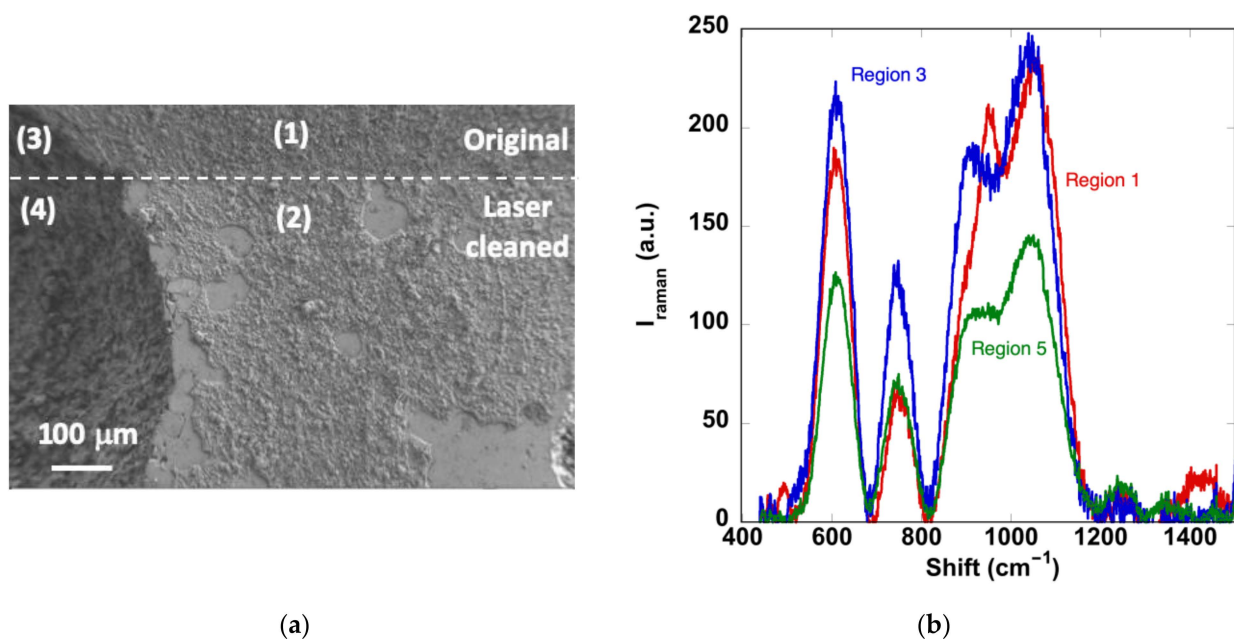
Figure 7. (**a**) FESEM image of the upper border of the laser-cleaned area in Region 3. The dashed line indicates the end of the laser-cleaned area. Points 1 to 4 indicate the positions where the EDS analysis reported in Table 3 was performed. (**b**) Raman spectra measured in three regions. The measurements in Regions 1 and 3 were performed in pitting areas, while the measurement in Region 5 was performed on the surface of the glass that was closest to the border of the sample. The latter appears to have undergone a distinct degradation process.

The EDS analysis (Table 5) was performed in the four points indicated in Figure 7, on both sides of the border between the original and the laser-cleaned region. Points 1 and 2 were selected on the crust over the glass surface and Points 3 and 4 on the pitting crater. The results suggest a strong reduction in the C content and that the laser cleaning

protocol eliminates the carbon contaminant layer. In addition, K was only detected within the laser-cleaned areas.

Table 5. EDS analysis (%at) of the composition measured in Region 3 of Figure 6 within the laser-cleaned stained-glass surface. The measurements were performed within 350 μm × 100 μm areas in the positions indicated in Figure 7a.

| % at	C	O	Si	Ca	K	Al	Mg	Fe	Pb	S	P
No laser (7.1)	45.7	43.2	6.7	1.0		1.1	0.3	1.2	0.2	0.4	
Cleaned (7.2)	5.8	63.0	25.1	1.1	0.4	2.6	0.6	1.4			
Pitting no laser (7.3)	49.4	42.2	4.4	1.9		0.9	0.3			0.9	
Pitting cleaned (7.4)	6.3	56.8	31.3	2.5	0.4	1.5				1.1	

Figure 8 presents some characteristics of the cleaned surfaces in a similar way to Figure 3 for the original surface and Figure 5 for the chemically cleaned surface. Figure 8a shows the surface of the pitting region with a magnification of 1500×. This region exhibits some positions where the particles appear to have been stripped. On the glass surface in the regions that are not affected by pitting (Figure 8b with a magnification of 500×), the amount of crust that is removed from the glass surface increases in comparison to the original surface, in a similar fashion to chemical cleaning. In addition, laser irradiation increased the number of glass substrate areas where the crust layer had been removed. The latter shows that the required laser irradiance is below the substrate surface's damage threshold. These surfaces appear flat and without damage, generated as a consequence of the laser irradiation treatment.

(**a**)   (**b**)
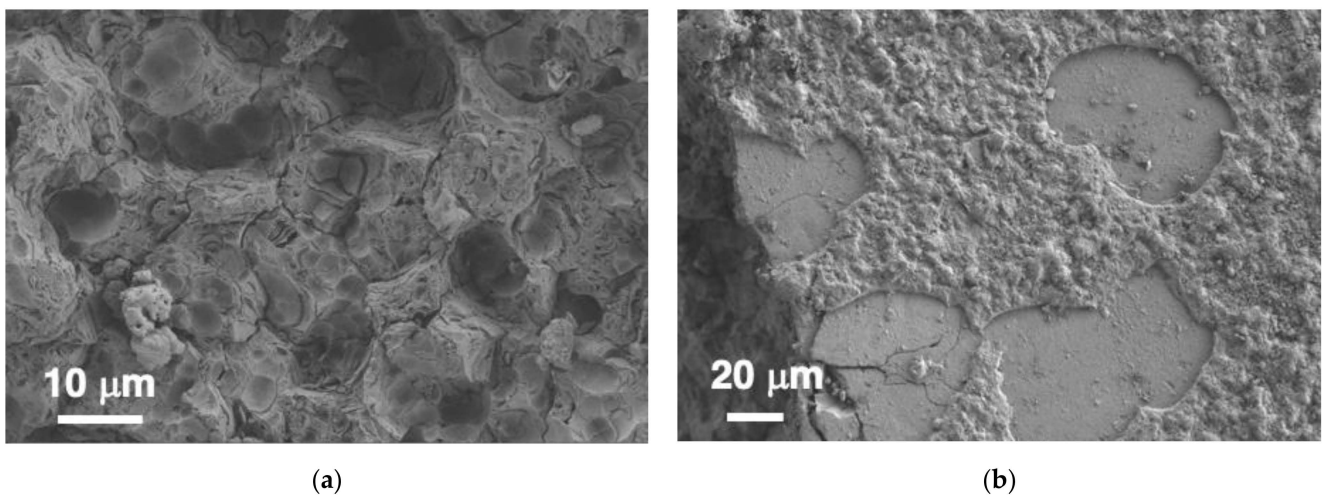
Figure 8. FESEM images of (**a**) a surface inside a crater and (**b**) of the upper glass in Region 3 after laser cleaning. The magnification is the same as in Figures 3 and 5.

Following the positive results observed in these initial laser cleaning processes, subsequent laser cleaning protocols were performed on some regions where the pitting was much deeper. To avoid any damage to the glass, the number of irradiation scans in each loop was limited to 20 in Regions 4 and 5. In the latter region, the main treated area corresponded to a region of the stained glass where the pitting effects were not observed. The FESEM micrographs presented in Figure 9 show the outline of the area that was laser-cleaned with 20 irradiation scans in Region 5 of Figure 6. The laser treatment was apparently enough to eliminate the contaminant layer present on top of the glass surface without deteriorating the original substrate. The cleaned glass surface exhibited a significant improvement in the transparency and no signs of melting, the formation of micro-cracks, nor any form of

laser induced damage. The laser-cleaned region exhibited a thin crust-like surface that could originate as a result of the mineral dynamics of the glass during leaching. A similar result was obtained by increasing the number of irradiation scans up to 50 (Region 6 in Figure 6). The substrate's integrity was preserved in this case, accompanied by a significant improvement in the glass transparency.

(**a**)   (**b**)
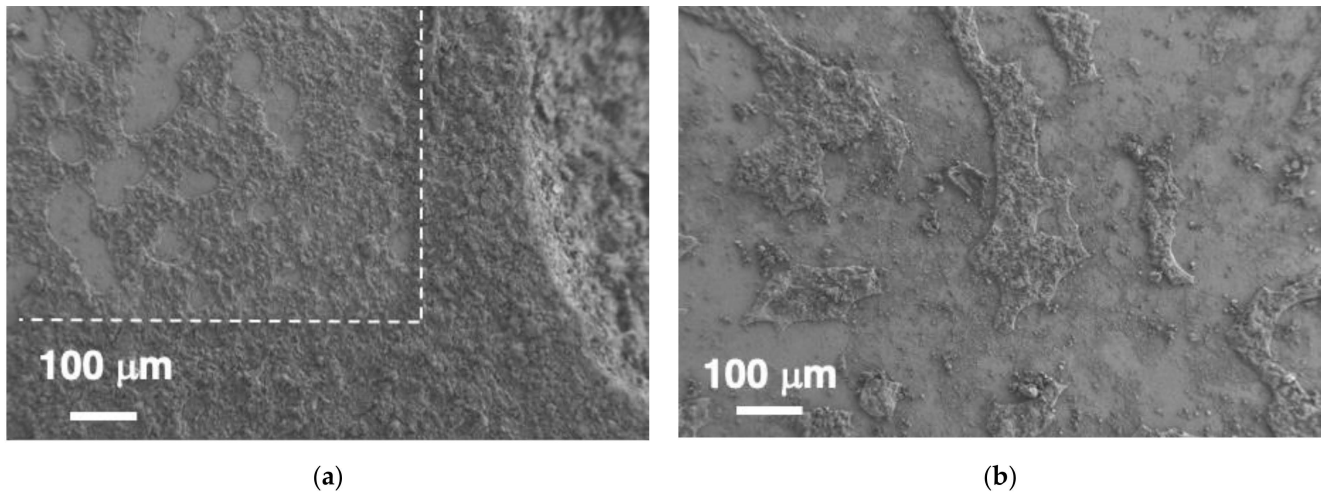
Figure 9. FESEM images of (**a**) the border and (**b**) the centre of Region 5 after applying a 20-scan laser cleaning protocol.

4. Discussion

Due to the nature of the potash-lime–silica glasses, the most common pathology observed on their surface is related to its alteration by dissolution. In this process, pitting defects are generated and appear covered with a white layer that contains the dissolved elements after the reaction with the atmosphere. Usually this surface is covered with a crust layer of black carbon contaminants. The chemical and laser cleaning protocols were demonstrated to be effective in the elimination of this external black layer and the outer part of the crust associated with the corrosion products, but both exhibit some limitations.

Chemical cleaning is a well-established restauration process, but it requires the use of chemicals which cause problems with the generation of waste, rinsing, deposits and their manipulation. Legislations are limiting the number of allowed chemicals, and this has to be considered. By contrast, laser cleaning is a more environmentally friendly technique.

The efficiency of chemicals is limited by their reaction with the white crust layer. In the cleaning of these stained-glass pathologies, it was established that the cleaning process is only efficient in the initial two or three applications. After that, the efficiency of the EDTA solution is strongly reduced. By contrast, the laser cleaning protocol allows for the fine tuning of the layer that is being ablated. One important problem associated with laser cleaning in these materials is that the crust layer and glass damage thresholds are very similar and require precise control of the removed layer. Moreover, these historic materials are not uniform and the optimum laser processing parameters need to be adjusted for each region of the surface with a different contaminant layer thickness or composition. In consequence, it is important to incorporate non-contact monitoring devices that will help improve cleaning process safety. Although the laser scans the complete surface in this work, recent developments are opening new possibilities for the combination of laser cleaning with in-situ optical and acoustic characterization methods. Further improvements may use artificial intelligence tools to adjust the laser parameters locally, depending on the characteristics of the surface in each spot. For the problem addressed in this study, the latter can be used to define different protocols in the regions where the glass has suffered from different levels of degradation.

It is also important to estimate the time required to perform these cleaning processes. In the case of chemical cleaning, the process herein applied required, on average, two or three repetitions with a duration of approximately 2.5 h per cycle, including the time for rinsing and cleaning. This gives a total processing time of approximately 5–6 h. Considering that several samples can be processed in parallel, it is reasonable to estimate that the cleaning of 3 m^2 may be achieved within this period of time. In the case of laser cleaning, the time required for a scan with the processing conditions used in this work was 44 s/cm^2. Assuming that a satisfactory laser cleaning process needs 100 scans, the required cleaning time becomes 1.2 h/cm^2. The process speed can be increased by increasing the size of the laser beam, because it allows for an increase in the laser scanning speed and the distance between the lines maintaining similar values of fluence or irradiance. For instance, with a laser spot three times larger, it is possible to clean an area of 1 m^2 in 13 h.

5. Conclusions

The chemical and laser cleaning procedures yielded similar results when applied to a potash-lime–silica glass that suffered from a strong degradation process due to glass dissolution. The sample exhibited a black layer of carbon contaminants that was easily removed from the sample surface in the initial cleaning stages. The observed increase in the Raman band intensity revealed that the laser cleaning process removed the external layer of the corrosion crust, leading to a flatter glass substrate surface. This was also observed in the pitting regions after laser cleaning.

This study has also shown that removing the encrustation to a satisfactory level using chemical cleaning requires the use of two or three EDTA cycles or a multi-scan laser irradiation process with at least 50 scans. In both cases, it was observed that when the cleaning process was applied to eliminate the contaminant encrustation layer that appeared on top of flat glass surfaces, the number of crust particles that were removed increased, producing flatter surfaces.

The comparison of the processing times highlights the fact that the chemical route is faster than laser cleaning. The latter avoids all the environmental problems associated with the use of harsh chemicals and the generation of unwanted residues, so that it offers a very desirable advantage which may compensate for its slower turnout.

Conflicts of Interest: The authors declare no conflict of interest. The funders had no role in the design of the study; in the collection, analyses or interpretation of data; in the writing of the manuscript or in the decision to publish the results.

References

1. Altavilla, C.; Ciliberto, E.; La Delfa, S.; Panarello, S.; Scandurra, A. The Cleaning of Early Glasses: Investigation about the Reactivity of Different Chemical Treatments on the Surface of Ancient Glasses. *Appl. Phys. A* **2008**, *92*, 251–255. [CrossRef]
2. Abd-Allah, R. Chemical Cleaning of Soiled Deposits and Encrustations on Archaeological Glass: A Diagnostic and Practical Study. *J. Cult. Herit.* **2013**, *14*, 97–108. [CrossRef]
3. Murcia-Mascarós, S.; Foglia, P.; Santarelli, M.L.; Roldán, C.; Ibañez, R.; Muñoz, A.; Muñoz, P. A New Cleaning Method for Historic Stained Glass Windows. *J. Cult. Herit.* **2008**, *9*, e73–e80. [CrossRef]
4. Römich, H.; Mottner, P.; Hildenhagen, J.; Dickmann, K.; Hettinger, G.; Bornschein, F. Comparison of Cleaning Methods for Stained Glass Windows. In *Lasers in the Conservation of Artworks*; Dickmann, K., Fotakis, C., Asmus, J.F., Eds.; Springer Proceedings in Physics; Springer: Berlin/Heidelberg, Germany, 2005; pp. 157–161. [CrossRef]
5. Römich, H.; Dickmann, K.; Mottner, P.; Hildenhagen, J.; Müller, E. Laser Cleaning of Stained Glass Windows—Final Results of a Research Project. *J. Cult. Herit.* **2003**, *4* (Suppl. 1), 112–117. [CrossRef]
6. Striova, J.; Fontana, R.; Barbetti, I.; Pezzati, L.; Fedele, A.; Riminesi, C. Multisensorial Assessment of Laser Effects on Shellac Applied on Wall Paintings. *Sensors* **2021**, *21*, 3354. [CrossRef]
7. Delgado, J.M.; Nunes, D.; Fortunato, E.; Laia, C.A.T.; Branco, L.C.; Vilarigues, M. The Effect of Three Luminescent Ionic Liquids on Corroded Glass Surfaces—A First Step into Stained-Glass Cleaning. *Corros. Sci.* **2017**, *118*, 109–117. [CrossRef]
8. Fekrsanati, F.; Klein, S.; Hildenhagen, J.; Dickmann, K.; Marakis, Y.; Manousaki, A.; Zafiropulos, V. Investigations Regarding the Behaviour of Historic Glass and Its Surface Layers towards Different Wavelengths Applied for Laser Cleaning. *J. Cult. Herit.* **2001**, *2*, 253–258. [CrossRef]
9. Carmona, N.; Villegas, M.A.; Fernández Navarro, J.M. Corrosion Behaviour of R_2O–CaO–SiO_2 Glasses Submitted to Accelerated Weathering. *J. Eur. Ceram. Soc.* **2005**, *25*, 903–910. [CrossRef]
10. Majérus, O.; Lehuédé, P.; Biron, I.; Alloteau, F.; Narayanasamy, S.; Caurant, D. Glass Alteration in Atmospheric Conditions: Crossing Perspectives from Cultural Heritage, Glass Industry, and Nuclear Waste Management. *NPJ Mater. Degrad.* **2020**, *4*, 27. [CrossRef]
11. Rodrigues, A.; Fearn, S.; Vilarigues, M. Historic K-Rich Silicate Glass Surface Alteration: Behaviour of High-Silica Content Matrices. *Corros. Sci.* **2018**, *145*, 249–261. [CrossRef]
12. Garcia-Vallès, M.; Gimeno-Torrente, D.; Martínez-Manent, S.; Fernández-Turiel, J.L. Medieval Stained Glass in a Mediterranean Climate: Typology, Weathering and Glass Decay, and Associated Biomineralization Processes and Products. *Am. Mineral.* **2003**, *88*, 1996–2006. [CrossRef]
13. Brill, R.H. Crizzling—A Problem in Glass Conservation. *Stud. Conserv.* **1975**, *20*, 121–134. [CrossRef]
14. Palomar, T.; Chabas, A.; Bastidas, D.M.; de la Fuente, D.; Verney-Carron, A. Effect of Marine Aerosols on the Alteration of Silicate Glasses. *J. Non-Cryst. Solids* **2017**, *471*, 328–337. [CrossRef]
15. Hench, L.L. Physical Chemistry of Glass Surfaces. *J. Non-Cryst. Solids* **1977**, *25*, 343–369. [CrossRef]
16. Vilarigues, M.; Redol, P.; Machado, A.; Rodrigues, P.A.; Alves, L.C.; da Silva, R.C. Corrosion of 15th and Early 16th Century Stained Glass from the Monastery of Batalha Studied with External Ion Beam. *Mater. Charact.* **2011**, *62*, 211–217. [CrossRef]
17. Gentaz, L.; Lombardo, T.; Loisel, C.; Chabas, A.; Vallotto, M. Early Stage of Weathering of Medieval-like Potash–Lime Model Glass: Evaluation of Key Factors. *Environ. Sci. Pollut. Res.* **2011**, *18*, 291–300. [CrossRef]
18. Dal Bianco, B.; Bertoncello, R.; Milanese, L.; Barison, S. Glass corrosion across the alps: A surface study of chemical corrosion of glasses found in marine and ground environments. *Archaeometry* **2005**, *47*, 351–360. [CrossRef]
19. Melcher, M.; Schreiner, M. Leaching Studies on Naturally Weathered Potash-Lime–Silica Glasses. *J. Non-Cryst. Solids* **2006**, *352*, 368–379. [CrossRef]
20. Krumbein, W.E.; Urzì, C.E.; Gehrmann, C. Biocorrosion and Biodeterioration of Antique and Medieval Glass. *Geomicrobiol. J.* **1991**, *9*, 139–160. [CrossRef]
21. Gorbushina, A.A.; Palinska, K.A. Biodeteriorative Processes on Glass: Experimental Proof of the Role of Fungi and Cyanobacteria. *Aerobiologia* **1999**, *15*, 183–192. [CrossRef]
22. Lombardo, T.; Ionescu, A.; Lefèvre, R.A.; Chabas, A.; Ausset, P.; Cachier, H. Soiling of Silica-Soda-Lime Float Glass in Urban Environment: Measurements and Modelling. *Atmos. Environ.* **2005**, *39*, 989–997. [CrossRef]
23. Kontozova-Deutsch, V.; Deutsch, F.; Godoi, R.H.M.; Van Grieken, R.; De Wael, K. Urban Air Pollutants and Their Micro Effects on Medieval Stained Glass Windows. *Microchem. J.* **2011**, *99*, 508–513. [CrossRef]
24. Valinoti, A.; Neves, B.; da Silva, E.; Maia, L. Surface Degradation of Composite Resins by Acidic Medicines and PH-Cycling. *J. Appl. Oral Sci. Rev. FOB* **2008**, *16*, 257–265. [CrossRef]
25. Tournié, A.; Ricciardi, P.; Colomban, P. Glass Corrosion Mechanisms: A Multiscale Analysis. *Solid State Ion.* **2008**, *179*, 2142–2154. [CrossRef]
26. Iglesias-Campos, M.A. Effects of Mechanical Cleaning by Manual Brushing and Abrasive Blasting on Lime Render Coatings on Architectural Heritage. *Mater. Constr.* **2014**, *64*, e039. [CrossRef]

27. Ibrahim, H.I.; Hamoudi, W.K.; Edan, M.S. Nanosecond Nd: YAG Laser Surface Cleaning of Metals and Marbles. *Iraqi J. Laser* **2015**, *14*, 21–26.
28. Pouli, P.; Paun, I.-A.; Bounos, G.; Georgiou, S.; Fotakis, C. The Potential of UV Femtosecond Laser Ablation for Varnish Removal in the Restoration of Painted Works of Art. *Appl. Surf. Sci.* **2008**, *254*, 6875–6879. [CrossRef]
29. Nevin, A.; Pouli, P.; Georgiou, S.; Fotakis, C. Laser Conservation of Art. *Nat. Mater.* **2007**, *6*, 320–322. [CrossRef]
30. Teule, R.; Scholten, H.; van den Brink, O.F.; Heeren, R.M.A.; Zafiropulos, V.; Hesterman, R.; Castillejo, M.; Martín, M.; Ullenius, U.; Larsson, I.; et al. Controlled UV Laser Cleaning of Painted Artworks: A Systematic Effect Study on Egg Tempera Paint Samples. *J. Cult. Herit.* **2003**, *4*, 209–215. [CrossRef]
31. Miller, J.C. 1. Introduction to Laser Desorption and Ablation. In *Laser Ablation and Desorption*; Miller, J.C., Haglund, R.F., Eds.; Experimental Methods in the Physical Sciences; Academic Press: Cambridge, MA, USA, 1997; Volume 30, pp. 1–13. [CrossRef]
32. Siano, S.; Agresti, J.; Cacciari, I.; Ciofini, D.; Mascalchi, M.; Osticioli, I.; Mencaglia, A.A. Laser Cleaning in Conservation of Stone, Metal, and Painted Artifacts: State of the Art and New Insights on the Use of the Nd:YAG Lasers. *Appl. Phys. A* **2012**, *106*, 419–446. [CrossRef]
33. Esbert, R.M.; Grossi, C.M.; Rojo, A.; Alonso, F.J.; Montoto, M.; Ordaz, J.; de Andrés, M.C.P.; Escudero, C.; Barrera, M.; Sebastián, E.; et al. Application Limits of Q-Switched Nd:YAG Laser Irradiation for Stone Cleaning Based on Colour Measurements. *J. Cult. Herit.* **2003**, *4*, 50–55. [CrossRef]
34. Maingi, E.M.; Alonso, M.P.; Angurel, L.A.; Rahman, M.A.; Chapoulie, R.; Dubernet, S.; de la Fuente, G.F. Historical Stained-Glass Window Laser Preservation: The Heat Accumulation Challenge. *Bol. Soc. Esp. Ceram. Vidr.* **2022**, *61*, S69–S82. [CrossRef]
35. Rahman, M.A.; de la Fuente, G.F.; Carretero, J.M.; Maingi, E.M.; Alonso Abad, M.P.; Alonso Alcalde, R.; Chapoulie, R.; Schiavon, N.; Angurel, L.A. Sub-Ns-Pulsed Laser Cleaning of an Archaeological Bone from the Sierra de Atapuerca, Spain: A Case Study. *SN Appl. Sci.* **2021**, *3*, 865. [CrossRef]
36. Lahoz, R.; Angurel, L.A.; Brauch, U.; Estepa, L.C.; de la Fuente, G. Laser Applications in the Preservation of Cultural Heritage: An Overview of Fundamentals and Applications of Lasers in the Preservation of Cultural Heritage. In *Con-Servation Science for the Cultural Heritage: Applications of Instrumen*; Varella, E.A., Ed.; Springer: Berlin/Heidelberg, Germany, 2013; pp. 294–332. [CrossRef]
37. Maingi, E.M. Laser Based Intervention in Historical Stained-Glasses. Ph.D. Thesis, University of Burgos, Burgos, Spain, University of Bordeaux Montaigne, Bordeaux, France, 2022.
38. Papanikolaou, A.; Siozos, P.; Philippidis, A.; Melessanaki, K.; Pouli, P. *Towards the Understanding of the Two Wavelength Laser Cleaning in Avoiding Yellowing on Stonework: A Micro-Raman and LIBS Study*; Nicolaus Copernicus University Press: Toruń, Poland, 2017; pp. 95–104. [CrossRef]
39. Vergès-Belmin, V.; Rolland, O.; Jourd'heuil, I.; Guiavarc'h, M.; Zanini, A. Nd:YAG Long Q-Switched versus Short Free-Running Laser Cleaning Trials at Chartres Cathedral, France. *Stud. Conserv.* **2015**, *60*, S12–S18. [CrossRef]
40. Zanini, A.; Trafeli, V.; Bartoli, L. The Laser as a Tool for the Cleaning of Cultural Heritage. *IOP Conf. Ser. Mater. Sci. Eng.* **2018**, *364*, 012078. [CrossRef]
41. Fekrsanati, F.; Hildenhagen, J.; Dickmann, K.; Troll, C.; Drewello, U.; Olaineck, C. UV-Laser Radiation: Basic Research of the Potential for Cleaning Stained Glass. *J. Cult. Herit.* **2000**, *1*, S155–S160. [CrossRef]
42. Römich, H.; Weinmann, A. Laser Cleaning of Stained Glass Windows. Overview on an Interdisciplinary Project. *J. Cult. Herit.* **2000**, *1*, S151–S154. [CrossRef]
43. Ueda, M.; Makino, R.; Kagawa, K.; Nishiyama, B. Laser Cleaning of Glass. *Opt. Lasers Eng.* **1991**, *15*, 275–278. [CrossRef]
44. Matteini, M.; Lalli, C.; Tosini, I.; Giusti, A.; Siano, S. Laser and Chemical Cleaning Tests for the Conservation of the Porta Del Paradiso by Lorenzo Ghiberti. *J. Cult. Herit.* **2003**, *4*, 147–151. [CrossRef]
45. Drewello, U.; Weißmann, R.; Rölleke, S.; Müller, E.; Wuertz, S.; Fekrsanati, F.; Troll, C.; Drewello, R. Biogenic Surface Layers on Historical Window Glass and the Effect of Excimer Laser Cleaning. *J. Cult. Herit.* **2000**, *1*, S161–S171. [CrossRef]
46. Echlin, M.P.; Straw, M.; Randolph, S.; Filevich, J.; Pollock, T.M. The TriBeam System: Femtosecond Laser Ablation in Situ SEM. *Mater. Charact.* **2015**, *100*, 1–12. [CrossRef]
47. Wu, J.; Zhang, Y.; Li, L.; Ren, Y.; Lu, Q.; Wang, L.; Chen, F. Raman Spectra Study on Modifications of BK7 Glass Induced by 1030-nm and 515-nm Femtosecond Laser. *Results Phys.* **2021**, *21*, 103814. [CrossRef]
48. Pouli, P.; Bounos, G.; Georgiou, S.; Fotakis, C. Femtosecond Laser Cleaning of Painted Artefacts; Is This the Way Forward? In *Lasers in the Conservation of Artworks*; Nimmrichter, J., Kautek, W., Schreiner, M., Eds.; Springer: Berlin/Heidelberg, Germany, 2007; pp. 287–293.
49. Zhang, H.; Eaton, S.M.; Li, J.; Herman, P.R. Heat Accumulation during High Repetition Rate Ultrafast Laser Interaction: Waveguide Writing in Borosilicate Glass. *J. Phy. Conf. Ser.* **2007**, *59*, 682–686. [CrossRef]
50. Weber, R.; Graf, T.; Berger, P.; Onuseit, V.; Wiedenmann, M.; Freitag, C.; Feuer, A. Heat Accumulation during Pulsed Laser Materials Processing. *Opt. Express* **2014**, *22*, 11312. [CrossRef]
51. Silverson. Dispersion and Hydration of Carbopol. Available online: https://www.silverson.com/us/resource-library/application-reports/dispersion-and-hydration-of-carbopol (accessed on 1 February 2023).
52. C.T.S. España S.L. Available online: https://shop-espana.ctseurope.com/234-carbogel (accessed on 1 February 2023).

53. Tomasini, E.P.; Gómez, B.; Halac, E.B.; Reinoso, M.; Di Liscia, E.J.; Siracusano, G.; Maier, M.S. Identification of Carbon-Based Black Pigments in Four South American Polychrome Wooden Sculptures by Raman Microscopy. *Herit. Sci.* **2015**, *3*, 19. [CrossRef]

54. Robinet, L.; Neff, D.D.; Bouquillon, A.; Pagès-Camagna, S.; Verney-Carron, A.; Etcheverry, M.-P.; Tate, J. Raman Spectrometry, a Non-Destructive Solution to the Study of Glass and Its Alteration. *Glass Ceram.* **2008**, *1*, 190–197.